Mathematical Biosciences and Engineering

MBE, 21(1): 1738–1764.
DOI: 10.3934/mbe.2024075
Received: 23 October 2023
Revised: 01 December 2023
Accepted: 11 December 2023
Published: 02 January 2024

http://www.aimspress.com/journal/MBE

Research article

A hybrid butterfly algorithm in the optimal economic operation of microgrids

Guohao Sun, Sen Yang, Shouming Zhang* and Yixing Liu

School of Information Engineering and Automation, Kunming University of Science and Technology, Kunming 650500, China

* **Correspondence:** Email: 595720558@qq.com.

Abstract: With the increasing capacity of renewable energy generators, microgrid (MG) systems have experienced rapid development, and the optimal economic operation is one of the most important and challenging issues in the MG field. To reduce the overall generation cost of microgrids, a hybrid butterfly algorithm (HBOA) is proposed to address the optimal economic operation problem in MG systems. This algorithm uses adaptive switching thresholds to balance the global exploration capability and local exploitation capability of the algorithm. It introduces a diversity learning mechanism to enhance information exchange among populations to improve the algorithm's accuracy and proposes an elite-guided guidance strategy to accelerate the convergence speed of the algorithm. Numerical simulation experiments on 10 standard test functions validate that the HBOA algorithm has higher optimization accuracy and faster convergence speed. Simulation experiments are conducted on two operation modes of microgrids: Islanded and grid-connected, and compared with other algorithms. In islanded and grid-connected modes, HBOA can reduce operating costs by up to 11.7% and 17.7%, respectively. The experimental results confirm the applicability and superiority of the proposed algorithm for solving the optimal economic operation problem in microgrids.

Keywords: microgrid; optimal economic operation; microgrid operation modes; hybrid butterfly algorithm

1. Introduction

To address the issues of traditional fossil fuel supply shortages and environmental pollution,

renewable energy sources such as tidal energy, wind energy, and solar energy are increasingly being deployed due to their advantages of being pollution-free, readily available and having low operational and maintenance costs [1]. Microgrid, as a small-scale distributed power distribution system, is a crucial component of the new power system. It can operate in grid-connected mode by connecting to the external power grid or autonomously in an isolated off-grid mode. Microgrids possess the characteristics of self-control and self-energy management [2,3]. Microgrid technology can not only improve the power supply quality in remote areas such as mountainous regions and islands but also, with a well-designed emergency energy dispatch strategy, reduce the losses incurred by power outages for users [4]. In this context, microgrid technology has emerged as a pioneer leading the transformation in the energy sector, providing a novel solution for the efficient management of energy systems.

Due to the diversity, multiple constraints and discontinuity inherent in the optimal economic operation models of microgrids [5], some traditional mathematical methods such as stochastic dynamic programming [6], stochastic linear programming [7], mixed-integer programming [8] and mixed-integer linear programming [9] struggle to yield satisfactory results. Therefore, population-based metaheuristic algorithms like particle swarm optimization [10], genetic algorithms [11,12], artificial bee colony algorithms [13], whale optimization algorithms [14] and other intelligent algorithms have been widely used to solve the problem of optimal economic operation in microgrids, owing to their powerful optimization capabilities. Almadhor et al. [15] proposed a hybrid particle swarm algorithm that introduced the frequency operator of the bat algorithm into the velocity update equation of the particle swarm algorithm to control speed, achieving better optimal solutions. It was successfully applied to solve the microgrid capacity allocation optimization problem with and without distributed energy sources. Li et al. [16] proposed a dual-layer optimization strategy to address the coordination of demand response and renewable energy generation in microgrids. They employed metaheuristic algorithms and mathematical methods to optimize the upper and lower layers separately, aiming to achieve optimal scheduling. This approach demonstrates high efficiency and computational speed. Chen et al. [17] proposed an improved shrimp algorithm, which enhanced convergence speed through a decreasing function. In the optimization and scheduling of microgrids containing photovoltaic units, their algorithm demonstrated superior performance compared to other algorithms.

Liu et al. [18] proposed an improved whale optimization algorithm that utilizes adaptive inertia weight and Levy flight trajectory strategy to enhance the algorithm's accuracy. This algorithm was verified to have superior performance in microgrid optimal planning simulation experiments.

The Butterfly Optimization Algorithm (BOA) takes inspiration from the foraging behavior of butterflies and was introduced by Arora et al. [19] for solving complex optimization problems. It has since been applied in various domains such as parameter identification [20], feature selection [21] and analog circuit design [22]. Addressing the drawbacks of BOA, such as susceptibility to local optima and slow convergence, Cai et al. [23] introduced a learning-based Butterfly Optimization Algorithm based on pinhole imaging. They designed an improved position update equation by introducing global optimum solutions and inertia weights to enhance the algorithm's optimization capability and solution accuracy. They employed an optical principle-based pinhole imaging learning strategy to avoid falling into local optima and demonstrated that this enhanced algorithm improves optimization accuracy on benchmark test functions. Long et al. [24] introduced velocity and memory terms during the local search phase to design a new position update equation. They also incorporated a refraction-based learning strategy to enhance algorithm diversity and exploratory capabilities. The improved Butterfly Algorithm showed significant superiority in solving high-dimensional functions.

The widespread application of metaheuristic algorithms has prompted deeper considerations for microgrid scheduling issues. These algorithms are not merely mathematical tools but rather flexible and powerful instruments capable of adapting to the dynamic changes and complexities within microgrid systems. Current research on microgrid scheduling issues places increased emphasis on the practical utility of algorithms, particularly focusing on achieving the optimal economic operation of microgrid systems in uncertain environments. However, the problem of optimal economic operation in microgrids is intricate and challenging, involving multiple interconnected factors such as energy supply and demand, equipment maintenance, and electricity price fluctuations.

For the microgrid optimal economic operation problem, we proposed a Hybrid Butterfly Algorithm (HBOA). HBOA uses adaptive switching thresholds to balance the algorithm's global exploration capability and local exploitation capability. we introduce a diversity learning mechanism to enhance information exchange among populations, thereby improving the algorithm's accuracy. Additionally, we proposed an elite-guided guidance strategy to accelerate the algorithm's convergence speed. Through numerical simulation experiments on 10 different standard test functions and simulation examples of optimal economic operation models in microgrids under both islanded and grid-connected operation modes, the feasibility and advancement of this algorithm in solving microgrid optimal economic operation problems have been validated.

Although some progress has been made in current efforts, the in-depth study of microgrid scheduling issues faces significant challenges. The crucial question of how to better integrate the innovation of metaheuristic algorithms with the practical operational requirements of microgrid systems remains a focal point in current research. Through a thorough analysis of the current research landscape, this paper aims to unveil the pivotal role of metaheuristic algorithms in addressing microgrid scheduling problems and provide a more profound insight into the future development of the microgrid field.

The first section of this paper elaborates on the current status and research significance of microgrid planning and operation. It introduces our ideas by highlighting some existing problems. The second section models various distributed micro-sources within the microgrid, providing their constraint equations and the expression for the operational cost of the microgrid. The third section provides a detailed explanation of the Standard Butterfly Optimization Algorithm, along with methods and strategies for its improvement. The fourth section conducts a comprehensive performance evaluation of the enhanced algorithm, presenting detailed results of the assessments. The fifth section establishes microgrid operational modes under different scenarios, validating the Hybrid Butterfly Optimization Algorithm's capability and robustness in addressing the optimal economic operation of microgrids through numerous case studies. The sixth section serves as a conclusion to summarize the work presented in this paper.

2. Problem description

With the objective of minimizing the overall system cost, this paper establishes a microgrid model that takes into account renewable energy, batteries and controllable microsources. Renewable energy includes wind energy (WT) and solar energy (PV), controllable micro-sources include diesel generators (DG) and micro gas turbines (MT), and the microgrid model is shown in Figure 1.

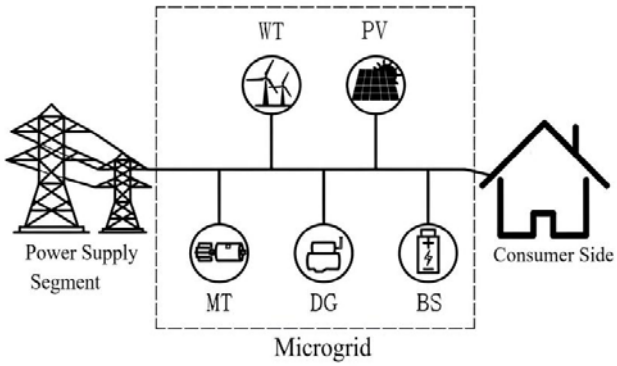

Figure 1. Microgrid model.

2.1. Microgrid model

The battery storage (BS) in a microgrid serves as an emergency backup power source, capable of responding rapidly and providing a certain amount of electrical energy in a short period to meet the power balance requirements of the microgrid [25]. The charging and discharging costs of the battery are as follows:

$$C(P_{BS}^t) = (P_{Bi}^t - P_{Bo}^t - \eta)B_d \tag{1}$$

In the equation, where P_{BS}^t is the power of BS at time t, P_{Bi}^t is the charging power of BS at time t, P_{Bo}^t is the discharging power of BS at time t, during charging $P_{Bo}^t = 0$ and during discharging $P_{Bi}^t = 0$; η represents the self-discharge power, and in the text, is taken as 0.2 kw. where B_d is cost coefficient.

Diesel generators (DG) have the advantage of rapid load adjustment. The operating costs of DG include fuel costs [26] and environmental pollution conversion costs, as shown in the following equations:

$$C(P_{DG}) = aP_{DG}^2 + bP_{DG} + c + \sum_{i=1}^{M} \beta_{DG}^i \gamma_{DG}^i P_{DG} \tag{2}$$

In the equation, where P_{DG} is the output power of DG; a, b, c are the cost coefficient of DG; M is type of pollutants, β_{DG}^i is the environmental pollution conversion coefficient for the i-th pollutant; γ_{DG}^i is the emissions of the i-th pollutant produced per unit of electricity generated by the DG.

Micro gas turbines (MT) can reduce environmental pollution emissions compared to traditional thermal power units. The operating costs of MT include fuel costs [27,28] and environmental pollution conversion costs, and their cost model is as follows:

$$C(P_{MT}) = \varphi\left(\frac{P_{MT}\Delta t}{\eta_{MT}}\right) + \sum_{i=1}^{M} \beta_{MT}^i \gamma_{MT}^i P_{MT} \tag{3}$$

In the equation, P_{MT} is the output power of the MT, φ is the natural gas price, Δt is unit operating time, in hours, η_{MT} is the MT's operating efficiency, assumed to be 80% in the text, β_{MT}^i is the environmental pollution conversion factor for the specific pollutant, γ_{MT}^i is the emission of the specific pollutant per unit electricity production by the MT.

2.2. Objective function

Islanded operation mode refers to the microgrid operating independently, without power exchange with the main grid, which is an important characteristic of the microgrid [29]. The components participating in islanded operation include WT, PV, DG, MT and BS, and their objective function is as follows:

$$\min F_c = \sum_{t=1}^{T}\sum_{j=1}^{U} C(P_j) + \sum_{t=1}^{T}\sum_{k=1}^{N} C(P_k) + \sum_{t=1}^{T} C(P_{BS}) \tag{4}$$

In the equation, where F_c is total cost of the microgrid system; where P_j is the actual output power of the j-th renewable energy source; where P_k is the actual output power of the k-th controllable microsource; where P_{BS} is the power for charging and discharging of the BS.

Grid-connected operation refers to the capability of the microgrid to exchange power with the main grid and control its operation according to market rules [30]. When the microgrid generates excess power, it can sell the surplus electricity to the main grid, and when the microgrid's generation is insufficient, it can draw power from the main grid. The components participating in grid-connected operation include WT, PV, DG, MT and BS, and their objective function is as follows:

$$\min F_c = \sum_{t=1}^{T}\sum_{j=1}^{U} C(P_j) + \sum_{t=1}^{T}\sum_{k=1}^{N} C(P_k) + \sum_{t=1}^{T} C(P_{BS}) + \sum_{t=1}^{T} C(P_L) \tag{5}$$

In the equation, where P_L is the power exchanged with the main grid.

2.3. Constraints

2.3.1. Power balance constraint:

$$P_{load} = \sum_{j=1}^{U} P_j + \sum_{k=1}^{N} P_k + P_{BS} + P_L \tag{6}$$

In the equation, where P_{load} is the load demand of the microgrid.

2.3.2. Controllable microsource power constraint:

$$P_k^{min} \le P_k \le P_k^{max} \tag{7}$$

In the equation, where P_k^{min} is the lower limit of the output power for the k-th controllable microsource; where P_k^{max} is the upper limit of the output power for the k-th controllable microsource.

2.3.3. Controllable microsource ramp rate constraint:

$$P_k^{low}\Delta t \le P_k(t) - P_k(t-1) \le P_k^{high}\Delta t \tag{8}$$

In the equation, where P_k^{low} is the upper limit of the ramp-down power for the k-th controllable microsource; P_k^{high} is the upper limit of the ramp-up power for the k-th controllable microsource.

2.3.4. Battery constraints:

$$P_{BS}^{min} \le P_{BS} \le P_{BS}^{max} \tag{9}$$

$$SOC^{low} \le SOC \le SOC^{high} \tag{10}$$

In the equation, where P_{BS}^{min} is the lower limit of the output power for the battery (BS); P_{BS}^{max} is the upper limit of the output power for the battery (BS); The state of charge (SoC) of the battery is the ratio of the current remaining capacity to the maximum capacity. To protect the battery as much as possible and extend its lifespan, the lower limit SOC^{low} and upper limit SOC^{high} of the battery's state of charge are established. In the text, SOC^{low} is set to 0.2, and SOC^{high} is set to 0.9.

2.3.5. Power constraint between the microgrid and the main grid:

$$P_L^{min} \le P_L \le P_L^{max} \tag{11}$$

In the equation, where P_L^{min} is the lower limit of power during power exchange; P_L^{max} is the upper limit of power during power exchange.

3. Hybrid butterfly algorithm

3.1. Standard butterfly optimization algorithm

Butterflies use their own sensors to locate the source of food. Each butterfly produces a certain concentration of fragrance, which spreads and is sensed by other butterflies in the search space. During the global search phase, butterflies are attracted to and move closer to other butterflies with a higher fragrance concentration than their own. During the local search phase, when a butterfly does not sense the fragrance of other butterflies, it moves randomly.

The fragrance concentration is described based on the physical intensity of the stimulus. The formula for calculating the fragrance concentration of a butterfly is as follows:

$$FP = c \times I^{\alpha} \tag{12}$$

In the equation, where c is perception factor, with an initial value of 0.01;α is power exponent, taken as 0.1 in the text; I is stimulus intensity, related to the fitness value.

During the global search phase, butterflies move towards the optimal solution, which can be expressed as:

$$X_i^{t+1} = X_i^t + (r^2 g^* - X_i^t) \times FP_i \tag{13}$$

In the equation, where X_i^t is the solution vector of the i-th butterfly in the t-th iteration; r is a random number between [0,1]; g^* is the current best solution vector up to that point; FP_i is the fragrance concentration of the i-th butterfly.

During the local search phase, butterflies undergo random walk, which can be expressed as:

$$X_i^{t+1} = X_i^t + \left(r^2 \times X_j^t - X_k^t\right) \times FP_i \tag{14}$$

In the equation, where X_i^t is randomly selected j-th butterfly; X_k^t is randomly selected k-th butterfly.

During the butterfly foraging process, whether butterflies perform global or local searches is determined by a switch threshold P, typically set to 0.8. In each iteration, a random number R between [0,1] is generated and compared to the switch threshold P. The final position update formula for the standard butterfly algorithm is as follows:

$$X_i^{t+1} = \begin{cases} X_i^t + (r^2 g^* - X_i^t)FP_i & , R \le P \\ X_i^t + (r^2 X_j^t - X_k^t)FP_i & , R > P \end{cases} \tag{15}$$

3.2. Hybrid butterfly algorithm

3.2.1. Adaptive switch threshold

The algorithm should focus on global search in the early iterations to maintain population diversity and switch to intensified local search in the later iterations to ensure population convergence. However, in Eq (15), the control switch threshold P = 0.8, which results in a high probability of the algorithm performing global search throughout the iterations. This makes it difficult to achieve a balance between global exploration and local exploitation, thereby reducing the convergence speed of the algorithm. Therefore, we adopt an adaptive switch threshold, allowing the value of P to adaptively adjust with the increase in the number of iterations. The values are as follows:

$$P = \left(\frac{T_{max} - t}{T_{max}}\right)^{\theta} \tag{16}$$

In the equation, where t is current iteration number; T_{max} is maximum number of iterations; θ is a parameter that linearly decreases from 2 to 1.

3.2.2. Diversity learning mechanism

Li [31] and others have summarized the regularities of many evolutionary algorithms and believe that 'the more effectively used information in evolutionary algorithms, the better the optimization performance of the algorithm'. In the standard butterfly algorithm, there is a lack of information exchange among individuals, leading to underutilization of effective information and limited precision in algorithm solutions. To address this issue, this paper proposes a diversity learning mechanism. After global search, individuals use the diversity learning mechanism to fully explore and utilize the effective information in the population to improve the algorithm's accuracy.

In the early stages of the algorithm, the population's average position is poor, and individuals are widely distributed in the search space. Each butterfly learns from the differences between the optimal butterfly position and the population's average position, effectively utilizing the population's useful information. This gradual improvement of the population's average position also leads to individuals becoming increasingly concentrated and moving towards the optimal solution area. The diversity

learning mechanism is as follows:

$$X_i^{t+1} = X_i^t + \text{Difference} \tag{17}$$

$$\text{Difference} = r_i(g^* - \lambda \times \text{Mean}) \tag{18}$$

$$\text{Mean} = \frac{1}{NP}\sum_{i=1}^{NP} X_i \tag{19}$$

In the equation, where Difference is diversity level;r_i is learning step size, $r_i \in [0,1]$; λ is learning factor, a random number between [1,2]; Mean is current population's average position; NP is population size.

3.2.3. Elite-guided guidance strategy

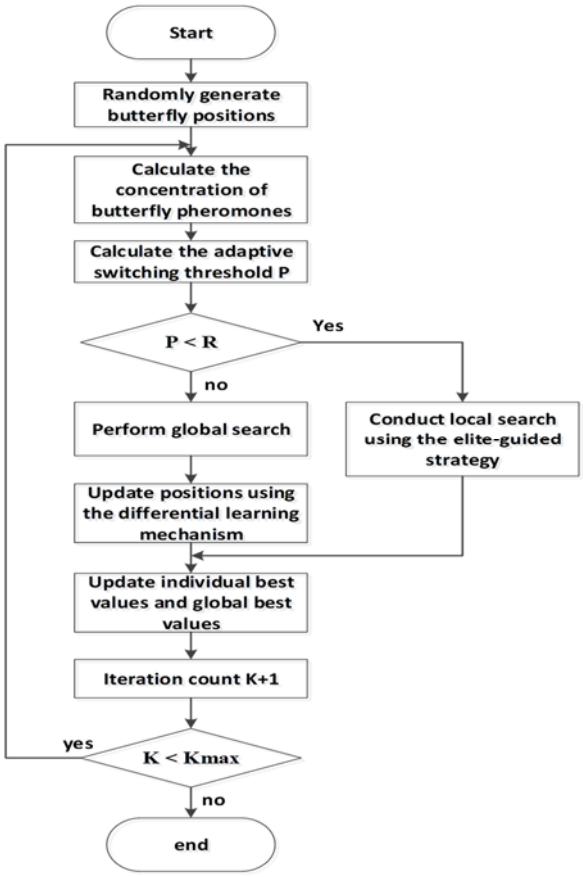

Figure 2. Flow chart of hybrid butterfly algorithm.

In the local search phase, as seen from Eq (14), the algorithm randomly selects individuals for local search, making the search process highly random and blind, which can reduce the convergence speed of the algorithm. To prevent the algorithm from getting stuck in local optima and accelerate convergence, this paper uses an improved search equation with an elite-guided guidance strategy in the local search phase, as follows:

$$X_i^{t+1} = \frac{1}{3}\left(g^* + p_i^* + X_j^t\right) + \left(r^2 \times X_s^t - \omega \times X_k^t\right) \times FP_i \tag{20}$$

$$\omega = \frac{1}{2}\left(|g^* - X_i^t| + |p_i^* - X_i^t|\right) \tag{21}$$

In the equation, where p_i^* is historical best solution of the i-th butterfly; X_s^t is elite butterfly randomly selected from the top 10% of the population's best individuals.

The improved search equation using the elite-guided guidance strategy incorporates information from more individuals, enhancing the search capability. It balances the exploitation ability of g^*(the best solution found so far), the relatively strong exploration abilities of X_j^t and X_k^t and the exploitation ability and exploration ability of p_i^* .The final formula exhibits a more suitable exploitation capability, directing the search towards better directions.

The flowchart of the hybrid butterfly algorithm is shown in Figure 2.

3.3. Hybrid butterfly algorithm solution process

The process of solving the optimal economic operation problem of a microgrid using the HBOA algorithm is as follows:

Step 1: Initialization - Input parameters related to various microsources, load demands, electricity prices for each time period, and algorithm-related parameters.

Step 2: Generate initial solutions based on the constraints of various microsources.

Step 3: Calculate fragrance concentration based on Eq (12).

Step 4: Calculate the adaptive switch threshold P based on Eq (16).

Step 5: Check if P is less than a random number R. If it's less, proceed to Step 8; if not, execute Steps 6 and 7.

Step 6: Perform global search and update the positions of the butterflies based on Eq (13).

Step 7: Apply diversity learning based on Eqs (17)–(19) and update the positions of the butterflies again.

Step 8: Update butterfly positions using Eqs (20) and (21).

Step 9: Check if all inequality and equality constraints are satisfied. If not, restrict them within the feasible range.

Step 10: Update the individual best solutions for each butterfly and the local best solution of the objective function, obtaining the current global best solution.

Step 11: Check if the current iteration count is less than the maximum iteration count. If yes, increment the iteration count and return to Step 3; otherwise, proceed to Step 12.

Step 12: Output the global best solution of the objective function, which represents the system's minimum cost.

4. Algorithm testing and effectiveness analysis

4.1. Testing function verification

To validate the optimization capabilities of HBOA, this paper selects 10 different standard test functions and conducts optimization calculations. Among these functions, F_1 to F_6 are unimodal

functions, while F_7 to F_{10} are multimodal functions. The experiments calculate and compare their optimal values, worst values, average values and standard deviations to assess the algorithm's optimization performance. Table 1 lists the names, dimensions, types, search space limits, and extrema required for the simulation experiments. Table 2 provides the mathematical expressions for F_1–F_{10}, where F_1–F_3 are basic sum-of-squares functions, F_4 and F_5 are absolute value-based functions, F_6 is a polynomial-type function, F_7 and F_8 are combinations of trigonometric functions and power functions, and F_9 and F_{10} are combinations of composite functions and trigonometric functions. Here, "D" represents the dimensionality of the problem.

Table 1. Benchmark function.

Function	Name	Dimension	Type	Search Space Bounds	Extremum
F_1	Sphere	30	unimodal	[-100,100]	0
F_2	SumSquare	30	unimodal	[-10,10]	0
F_3	SumPower	30	unimodal	[-1,1]	0
F_4	Schwefel 2.22	10	unimodal	[-10,10]	0
F_5	Schwefel 2.21	30	unimodal	[-100,100]	0
F_6	Quartic	30	unimodal	[-1.28,1.28]	0
F_7	Rastrigin	30	multimodal	[-5.12,5.12]	0
F_8	Griewank	30	multimodal	[-600,600]	0
F_9	Ackley	30	multimodal	[-32,32]	0
F_{10}	Schaffer	2	multimodal	[-100,100]	0

Table 2. Function expression.

Function	Function Name	Expression
F_1	Sphere	$f(x) = \Sigma_{i=1}^{D} x_i^2$
F_2	SumSquare	$f(x) = \Sigma_{i=1}^{D} i \cdot x_i^2$
F_3	SumPower	$f(x) = \Sigma_{i=1}^{D} \lvert x_i \rvert^{i+1}$
F_4	Schwefel 2.22	$f(x) = max_i \lvert x_i \rvert$
F_5	Schwefel 2.21	$f(x) = \Sigma_{i=1}^{D} \lvert x_i \rvert + \Pi_{i=1}^{D} \lvert x_i \rvert$
F_6	Quartic	$f(x) = \Sigma_{i=1}^{D} i \cdot x_i^4 + rand(0,1)$
F_7	Rastrigin	$f(x) = 10D + \Sigma_{i=1}^{D} [x_i^2 - 10\cos(2\pi x_i)]$
F_8	Griewank	$f(x) = \frac{1}{4000} \sum_{i=1}^{D} x_i^2 - \Pi_{i=1}^{D} \cos\left(\frac{x_i}{\sqrt{i}}\right) + 1$
F_9	Ackley	$f(x) = -20\exp\left(-0.2\sqrt{\frac{1}{D}\Sigma_{i=1}^{D} x_i^2}\right) - \exp\left(\frac{1}{D}\Sigma_{i=1}^{D}\cos(2\pi x_i)\right) + 20 + \exp(1)$
F_{10}	Schaffer	$f(x) = 0.5 + \frac{\sin^2(x_1^2 - x_2^2) - 0.5}{[1 + 0.001(x_1^2 + x_2^2)]^2}$

4.2. Analysis of the effectiveness of improvement strategies

To analyze the impact of the three improvement strategies on algorithm performance, we compare HBOA with the Standard Butterfly Algorithm (BOA), algorithm that adaptive switch threshold (SBOA), algorithm that only uses the diversity learning mechanism (DBOA) and an algorithm that only uses the elite-guided guidance strategy (EBOA). The experiments selected test functions F_1, F_2, F_4 and F_8, set the population size to 50, and the maximum iteration count to 1000. The statistical results of 20 independent runs for each of the five algorithms are shown in Table 3.

Table 3. Comparison results of effectiveness of improvement strategies.

Function	Metric	BOA	SBOA	DBOA	EBOA	**HBOA**
F_1	Best	24.17	1.91	5.07E-191	7.28E-07	**0.00E+00**
	Worst	74.47	3.63	1.82E-173	8.37E-07	**0.00E+00**
	Mean	47.75	2.88	9.41E-175	7.83E-07	**0.00E+00**
	Std	13.19	0.43	0.00E+00	2.64E-08	**0.00E+00**
F_2	Best	11.77	0.95	1.39E-194	6.39E-07	**0.00E+00**
	Worst	22.93	1.74	3.67E-171	5.34E-07	**0.00E+00**
	Mean	17.68	1.37	1.84E-172	5.97E-07	**0.00E+00**
	Std	2.81	0.25	0.00E+00	2.81E-08	**0.00E+00**
F_4	Best	0.73	0.08	5.05E-99	3.49E-05	**0.00E+00**
	Worst	7.12	0.51	1.16E-86	6.76E-05	**0.00E+00**
	Mean	2.39	0.25	6.66E-88	5.23E-05	**0.00E+00**
	Std	1.44	0.13	2.59E-87	6.78E-06	**0.00E+00**
F_8	Best	1.25	5.42E-3	0.00E+00	1.06E-06	**0.00E+00**
	Worst	1.45	1.47E-2	0.00E+00	1.05	**0.00E+00**
	Mean	1.36	9.36E-3	0.00E+00	0.21	**0.00E+00**
	Std	5.63E-2	2.37E-3	0.00E+00	0.42	**0.00E+00**

From Table 3, it can be observed that using only the adaptive switch threshold provides limited improvement to the performance of the standard BOA. The diversity learning mechanism plays a dominant role in improving the performance of the standard BOA. The elite-guided guidance strategy directs the algorithm towards better directions, and when combined with the diversity learning mechanism, it fully exploits the effective information within the population, further enhancing the optimization accuracy and convergence speed of the standard BOA. Figure 3 provides the convergence curves for the four benchmark test functions.

To further validate the superiority of HBOA, it is compared with LHHO [32], ISMTSA [33], AIWSSA [34] and HPSOBOA [35]. The specific settings of control parameters for the other comparison algorithms can be found in the respective references. The population size is set to 50, and the maximum iteration count is 1000.The statistical results of 20 independent runs for each of the five algorithms are shown in Table 4.

From Table 4, it can be observed that in the optimization tests for unimodal functions F_1 to F_5, HBOA consistently finds the optimal values with a higher success rate compared to the other four algorithms. In the case of the unimodal test function F_6, five algorithms exhibit comparable optimization performance. In the optimization tests for multimodal functions F_7 to F_{10}, five

algorithms demonstrate commendable optimization accuracy.

To provide a more intuitive analysis of the convergence performance of these five algorithms, Figure 4 shows the convergence curves for some of the benchmark test functions. From Figure 4, it can be seen that on unimodal test function F_3,where only ISMTSA fails to find the optimal value, HBOA exhibits the fastest convergence speed. On multimodal test functions F_7, F_8, and F_{10}, all five algorithms can find the optimal values, HBOA shows the best convergence speed.

In summary, HBOA demonstrates superior performance in terms of both optimization accuracy and convergence speed, making it more competitive.

The data in Table 5 represents the time comparison for five algorithms across three scenarios. It can be observed that the average time consumed by HBOA is greater than that of the other algorithms. In comparison to the original algorithm, HBOA exhibits significantly improved accuracy, albeit at the cost of increased complexity and extended running time. However, sacrificing some efficiency to achieve higher accuracy is acceptable, and the additional time is justifiable for potential cost savings.

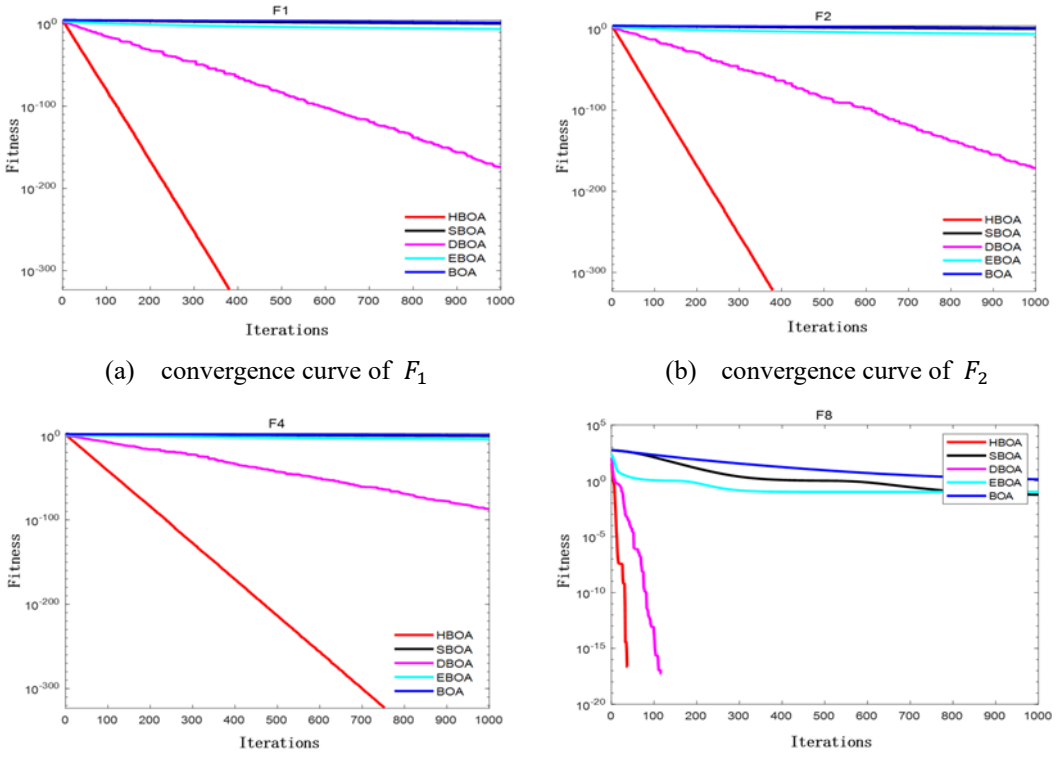

(a) convergence curve of F_1 (b) convergence curve of F_2

(c) convergence curve of F_4 (d) convergence curve of F_8

Figure 3. Convergence curves of different improved strategy algorithms.

Table 4. Function performance comparison results.

Function	Metric	NPWOA	ISMTSA	LHHO	HPSOBOA	**HBOA**
F_1	Best	1.82E-225	4.10E-60	4.66E-316	0	**0**
	Worst	2.35E-202	7.26E-83	1.42E-287	0	**0**
	Mean	1.17E-203	2.05E-61	8.07E-289	0	**0**
	Std	0	9.16E-61	0	0	**0**
F_2	Best	1.83E-227	1.04E-75	4.63E-309	0	**0**
	Worst	8.97E-207	2.20E-54	4.21E-282	0	**0**
	Mean	5.05E-208	2.20E-55	2.14E-283	0	**0**
	Std	0	6.41E-55	0	0	**0**
F_3	Best	0	1.70E-121	0	0	**0**
	Worst	0	5.08E-106	0	0	**0**
	Mean	0	4.63E-107	0	0	**0**
	Std	0	1.43E-106	0	0	**0**
F_4	Best	5.76E-137	2.29E-51	9.50E-167	2.13E-293	**0**
	Worst	3.25E-124	2.23E-45	1.83E-149	8.13E-293	**0**
	Mean	1.66E-125	1.68E-46	9.46E-151	5.63E-293	**0**
	Std	7.26E-125	4.96E-46	4.10E-150	0	**0**
F_5	Best	2.03E-38	1.62E-33	6.64E-157	3.27E-293	**0**
	Worst	2.08E-28	6.10E-10	2.08E-141	7.22E-293	**0**
	Mean	1.34E-29	3.06E-11	1.31E-142	5.58E-293	**0**
	Std	4.69E-29	1.36E-10	4.70E-142	0	**0**
F_6	Best	5.11E-05	2.72E-06	3.52E-06	1.17E-06	**2.26E-06**
	Worst	1.41E-03	4.28E-04	2.06E-04	1.04E-04	**6.86E-05**
	Mean	4.31E-04	8.89E-05	5.48E-05	4.29E-05	**2.28E-05**
	Std	3.69E-04	1.13E-04	5.58E-05	2.92E-05	**1.96E-05**
F_7	Best	0	0	0	0	**0**
	Worst	0	0	0	0	**0**
	Mean	0	0	0	0	**0**
	Std	0	0	0	0	**0**
F_8	Best	0	0	0	0	**0**
	Worst	0	0	0	0	**0**
	Mean	0	0	0	0	**0**
	Std	0	0	0	0	**0**
F_9	Best	8.88E-16	8.88E-16	8.88E-16	8.88E-16	**8.88E-16**
	Worst	7.99E-15	7.99E-15	8.88E-16	8.88E-16	**8.88E-16**
	Mean	4.09E-15	1.60E-15	8.88E-16	8.88E-16	**8.88E-16**
	Std	2.16E-15	1.72E-15	0	0	**0**
F_{10}	Best	0	0	0	0	**0**
	Worst	0	0	0	0	**0**
	Mean	0	0	0	0	**0**
	Std	0	0	0	0	**0**

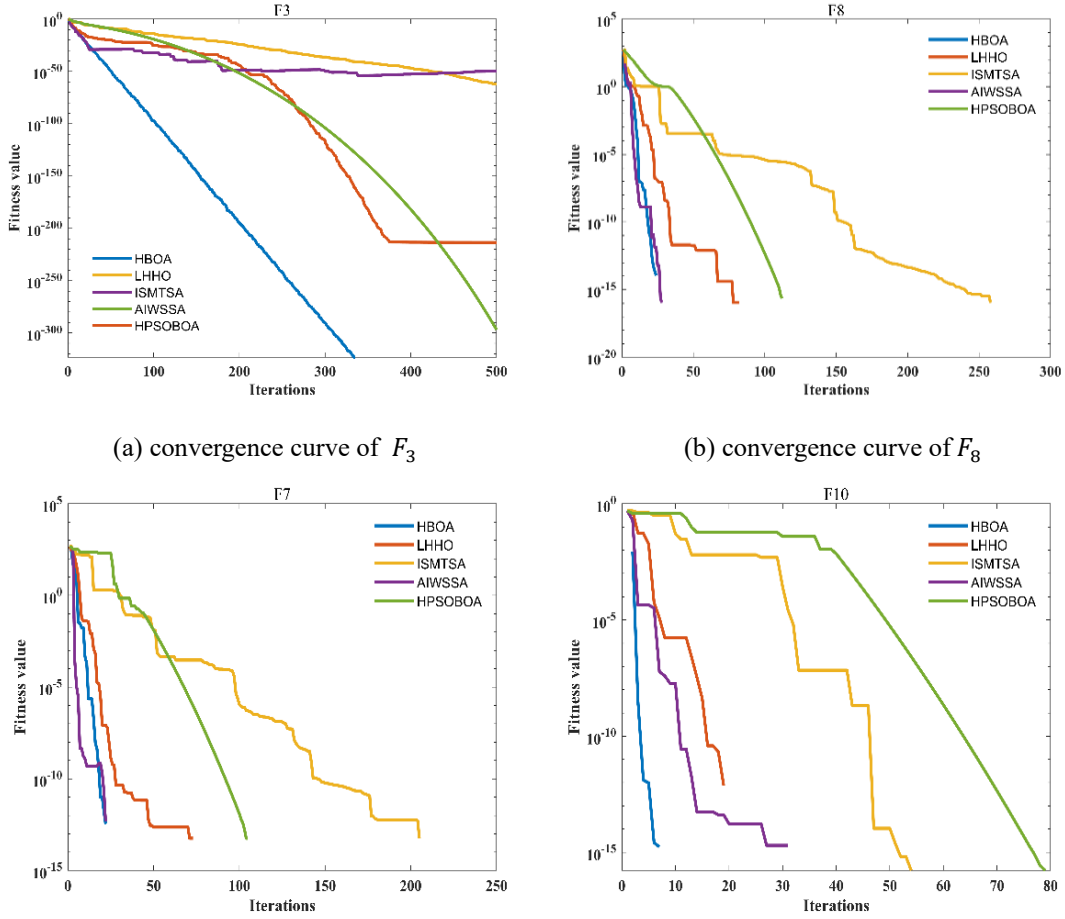

(a) convergence curve of F_3

(b) convergence curve of F_8

(c) convergence curve of F_7

(d) convergence curve of F_{10}

Figure 4. Convergence curves of partial test functions.

Table 5. The efficiency comparison results of five algorithms in different scenarios.

Scenarios	Time indicators/s	NPWOA	ISMTSA	LHHO	HPSOBOA	HBOA
Scenario 1	fastest	0.052907	0.065851	0.17253	0.10306	0.22448
	slowest	0.055274	0.071141	0.19057	0.10919	0.2286
	Mean	0.054169	0.067612	0.17741	0.10535	0.22688
Scenario 2	fastest	0.11729	0.12785	0.40536	0.14234	0.35663
	slowest	0.11916	0.13451	0.4296	0.14892	0.37614
	Mean	0.11837	0.13145	0.41507	0.14531	0.36385
Scenario 3	fastest	0.016614	0.029313	0.0537	0.030272	0.16509
	slowest	0.01823	0.031614	0.056324	0.032503	0.17392
	Mean	0.017269	0.030491	0.05521	0.03117	0.17004

5. Simulation results

In the optimal economic operation of the microgrid, WT (Wind Turbine) and PV (Photovoltaic) are renewable energy sources that do not directly participate in the optimal economic operation in this paper. Therefore, it is necessary to predict their power output. Then, the optimal economic operation of DG (Diesel Generator), MT (Micro Turbine), BS (Battery Storage), and the interaction power with the main grid is continuously optimized to achieve the goal of minimizing the total system cost. The optimal economic operation cycle is 24 hours with a time interval of 1 hour. The daily power forecasts [36] for WT, PV and load demand in a specific location are shown in Figures 5 and 6, respectively. The parameters [37] for each microsource and emission coefficients are listed in Table 6.

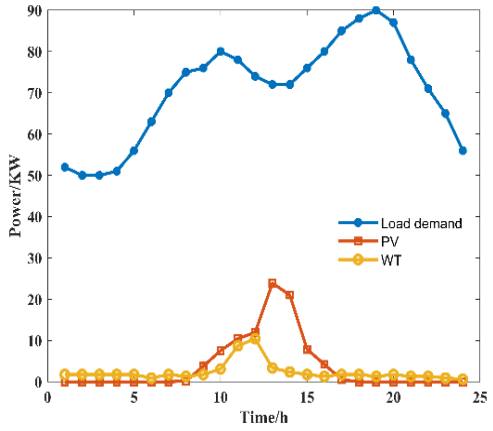

Figure 5. Load wind power photoelectric forecast power curve.

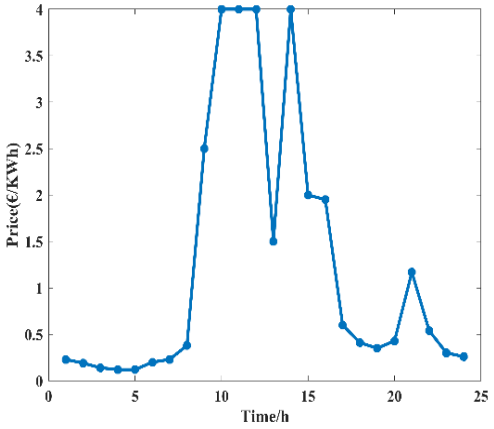

Figure 6. Time-of-use power price.

In this paper, the microgrid is operated in both islanded and grid-connected modes. To verify the applicability and superiority of HBOA in solving the optimal economic operation problem of microgrids, this algorithm is compared and analyzed separately for both operating modes with Particle Swarm Optimization (PSO), Standard Butterfly Algorithm (BOA), Improved Whale Optimization

Algorithm (IWAO) [18] and Hybrid ABC-PSO [38] (algorithm parameters referenced from the original literature). The actual output power of each microsource is also explained.

Table 6. Related parameters of micro power supply.

Type	P_{min}/KW	P_{max}/KW	Bid/€	CO_2 kg/MKW	SO_2 kg/MKW	NO_x kg/MKW
WT	0	15	1.073	0.000	0.000	0.000
PV	0	25	2.584	0.000	0.000	0.000
DG1	3	30	0.294	460.0	0.0030	0.0075
DG2	3	30	0.294	460.0	0.0030	0.0075
MT	6	30	0.457	720.0	0.0036	0.1000
BS	-30	30	0.380	10.00	0.0002	0.0001
Grid	-30	30	—	0.000	0.000	0.000

5.1. Islanded operation mode

Table 7 presents the best, worst, average values and standard deviations obtained from 20 independent runs of the algorithms. The average convergence curves of the five algorithms for microgrid islanded operation mode are shown in Figure 7. From Table 6 and Figure 7, it can be observed that IWOA has the fastest convergence speed, while HBOA is slightly slower but demonstrates a significant advantage in terms of optimization accuracy. HBOA outperforms IWOA, ABC-PSO, BOA, and PSO by 8.1%, 10.5%, 11.0% and 11.3%, respectively, in terms of optimization accuracy. Additionally, HBOA has the lowest standard deviation among the five algorithms, only 3.5, indicating higher solution stability.

Table 7. Comparison of results of 5 algorithms under island operation mode.

Algorithm	Metric	PSO	BOA	IWOA	ABCPSO	**HBOA**
Total system cost/€	Best	1045.7	1041.5	1012.1	1034.2	**932.4**
	Worst	1064.4	1057.9	1020.7	1048.2	**937.4**
	Mean	1053.0	1048.2	1016.4	1044.2	**934.9**
	Std	11.9	8.4	6.0	10.3	**3.5**

Figure 8 shows the scheduling results for different microsources at various time periods using HBOA in the islanded operation mode. It can be observed that:

From 1 to 9 hours, renewable energy sources are in a low-output period, and the load demand is low. Battery Storage (BS) releases some electrical energy, while diesel generators (DG) and Micro Turbines (MT) generate power to meet the power balance.

From 10 to 16 hours, renewable energy sources are in a high-output period, and the load demand is high. DG, which has lower costs, generates a significant amount of power, storing surplus electrical energy in BS and adjusting MT to achieve power balance.

During 17 to 24 hours, when renewable energy output is low but load demand remains high, BS releases stored energy, and DG generates a large amount of power. The output power of the more costly MT remains relatively unchanged while maintaining power balance.

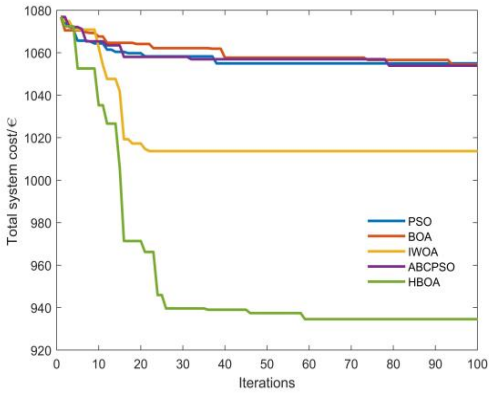

Figure 7. Iteration curve under island operation mode.

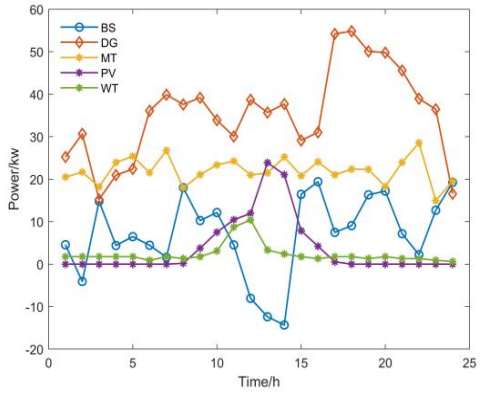

Figure 8. The result of power resources in island mode.

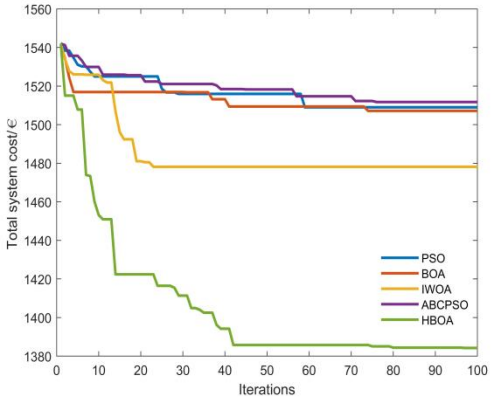

Figure 9. Iteration curve for the Islanded operation mode of a small commercial microgrid.

To validate the applicability of the algorithm, optimization scheduling was performed for a small-scale commercial microgrid under both islanded and grid-connected operation modes. Table 8 presents

the results of five algorithms running 20 times under the islanded operation mode. Analysis reveals that the Hybrid Butterfly Algorithm (HBOA) achieved the optimal result in the objective function, reaching 1384.165. Additionally, its average result is the smallest among the five algorithms. This indicates that HBOA exhibits superior search performance in this case, finding a favorable microgrid scheduling solution.

Figures 9 and 10 display the cost iteration curves and microsource dispatch results, respectively. A comparison shows that even with slightly higher commercial electricity prices and variations in the load curve and renewable energy output, HBOA can find a good solution. The detailed analysis of each microsource's output is not provided here.

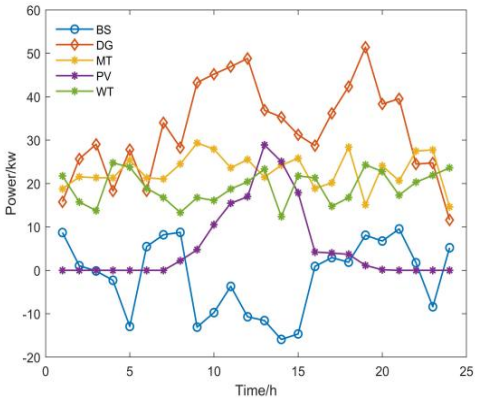

Figure10. Optimization results for microsource operation in the Islanded mode of a small commercial microgrid.

Table 8. Algorithmic results comparison for islanded operation in commercial microgrid.

Algorithm	Metric	PSO	BOA	IWOA	ABCPSO	**HBOA**
	Best	1501.9453	1505.3399	1473.8645	1507.4778	**1384.165**
Total system	Worst	1517.6527	1508.1062	1482.6351	1514.7994	**1384.3792**
cost/€	Mean	1508.9808	1507.1425	1478.1385	1511.7294	**1384.2364**
	Std	7.9805	1.5624	4.3895	3.8011	**0.12368**

5.2. Grid-connected operation mode

Table 9 presents the results obtained from 20 independent runs of the algorithms. The average convergence curves of the five algorithms for microgrid grid-connected operation mode are shown in Figure 11. In grid-connected mode, due to the connection with the main grid, surplus electrical energy can be sold to the main grid for revenue, further reducing the system's total cost. From Table 8 and Figure 11, it can be seen that HBOA achieves the highest solution quality, with an improvement in optimization accuracy of 12.3%, 15.5%, 14.0% and 17.7% compared to IWOA, ABC-PSO, BOA and PSO, respectively. Compared to the islanded operation mode, precision is further improved. IWOA

has a faster convergence speed but is more prone to getting stuck in local optima.

Table 9. Comparison of results of five algorithms in grid-connected mode.

Algorithm	Metric	PSO	BOA	IWOA	ABCPSO	**HBOA**
Total system cost/€	Best	557.0	545.3	505.2	531.9	**450.6**
	Worst	605.5	586.6	577.9	598.1	**502.8**
	Mean	579.3	554.6	543.9	564.2	**476.6**
	Std	32.2	28.3	36.5	33.1	**26.1**

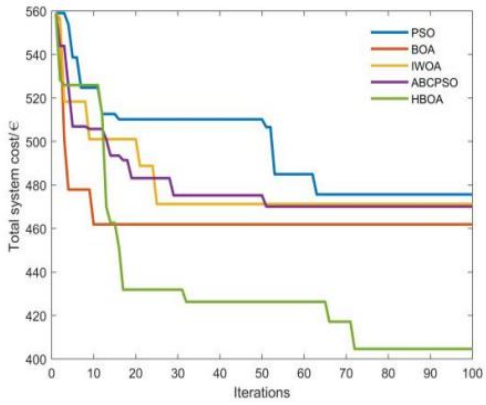

Figure 11. Iteration curve under grid-connected mode.

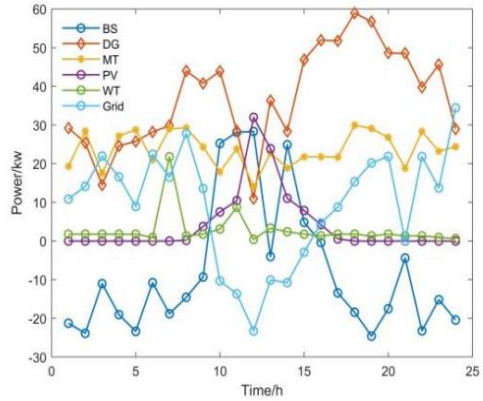

Figure 12. The result of power resources in grid-connected mode.

As it can interact with the main grid, a more stable power balance can be maintained within the microgrid. Figure 12 displays the scheduling results for different microsources at various time periods using HBOA in the grid-connected operation mode. Figures 13 and 14 illustrate the relationship between electricity prices and battery storage (BS) power at different time intervals and the interaction power with the main grid after optimization using HBOA, respectively.

It can be observed that, during the low-price periods from 1 to 8 hours, the microgrid absorbs a significant amount of electricity from the main grid at lower prices and stores some of it in BS.

In high-price periods at 10, 11, 12 and 14 hours, BS, which incurs lower pollution control costs, releases a large amount of electrical energy. The low-cost diesel generators (DG) generate more power, allowing the microgrid to supply a substantial amount of electricity to the main grid for higher returns.

During the low-price periods from 17 to 20 hours and 22 to 24 hours, BS releases a substantial amount of electrical energy. Since renewable energy output is relatively low, DG, with its lower costs, generates a significant amount of power. Micro Turbines (MT) are adjusted to meet the power balance constraints.

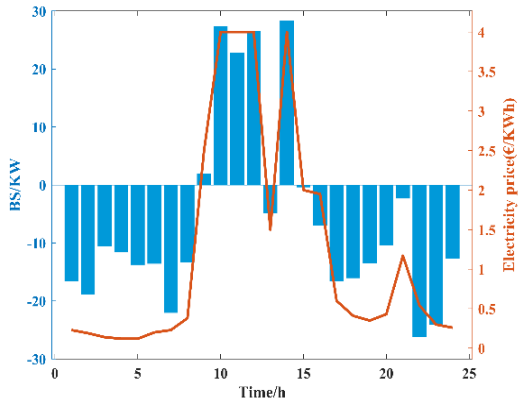

Figure 13. The relationship between electricity price and battery power.

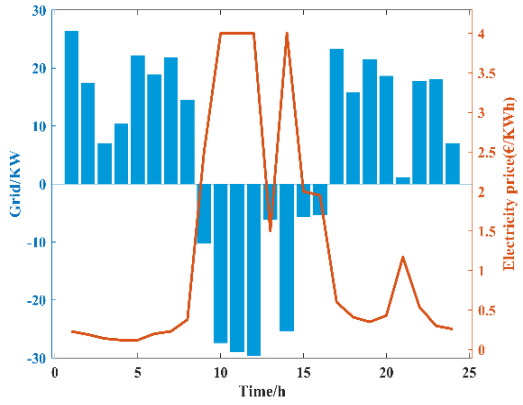

Figure 14. The relationship between the electricity price and the interactive power of the main grid.

Tables 7 and 9 reveal that the grid-connected operation mode, which allows power interaction with the main grid, leads to a reduction in the overall system cost compared to the islanded operation mode. In the grid-connected mode, electricity can be absorbed from the main grid when the selling prices are low, reducing the generation from controllable microsources, thus lowering the total system cost. Additionally, during high-price periods, increasing the generation from controllable microsources and exporting surplus energy to the main grid for revenue generation can further reduce the system's overall cost.

Table 10. Algorithmic results comparison for grid-connected operation in commercial microgrid.

Algorithm	Metric	PSO	BOA	IWOA	ABCPSO	**HBOA**
Total system cost/€	Best	892.9969	913.9616	894.6657	897.1126	**803.0668**
	Worst	939.542	934.5172	925.7031	927.152	**862.6087**
	Mean	912.9266	922.5338	906.5305	916.9885	**827.3853**
	Std	23.982	10.6939	16.7595	17.2145	**31.2329**

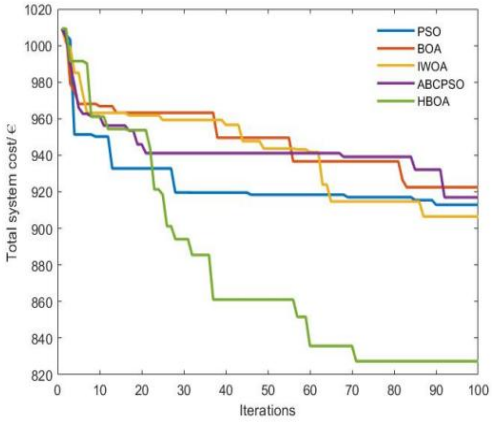

Figure 15. Iteration curve for the grid-connected operation mode of a small commercial microgrid.

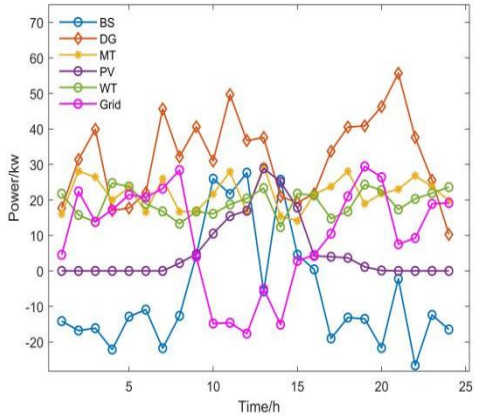

Figure 16. Optimization results for microsource operation in the grid-connected operation mode of a small commercial microgrid.

Table 10 presents the results of running five algorithms 10 times in the experiment of commercial microgrid operation. It is noteworthy that, in this scenario, the Hybrid Butterfly Optimization Algorithm (HBOA) stands out once again with outstanding performance, achieving remarkable optimal solutions and highlighting its superiority in microgrid scheduling problems. However, despite a relatively large standard deviation, indicating potential room for improvement in the search process, this cannot overshadow the excellent performance of HBOA in microgrid optimization. HBOA not only demonstrates exceptional optimal solutions but also excels in terms of worst-case solutions, showcasing its high level of stability. This outstanding stability positions HBOA as a reliable tool for

solving microgrid scheduling problems.

Figures 15 and 16 depict the cost iteration curve and micro-source scheduling results. During the period of low electricity prices from 1 to 8 o'clock, the microgrid charges the battery through power purchases. From 9 to 15 o'clock, when prices are higher, it coincides with the peak output period of renewable energy sources. To save costs, the microgrid increases the output of distributed generation (DG), discharges the battery, and sells excess electricity to generate additional revenue. After 18 o'clock, electricity prices decrease, and the photovoltaic output significantly decreases. The microgrid then purchases electricity at a lower cost, increases DG output, charges the battery as a reserve energy source to cope with the next load peak, and reduces overall costs.

To assess the flexibility of the algorithm, specifically its ability to adjust operational strategies to accommodate variations in load, photovoltaic (PV) and wind power fluctuations, the following experiments were conducted:

Load Fluctuation Test: Simulating sudden changes in the load within the microgrid, representing unexpected increases or decreases in load demand.

Renewable Energy Fluctuation Test: Simulating fluctuations in renewable energy sources (such as solar and wind energy) and scenarios where the supply of renewable energy is unstable.

Battery Uncertainty Test: Assessing the robustness of the algorithm in the face of fluctuations in charge-discharge efficiency, uncertainty in battery types, and other variations in battery performance.

Figure 17 depicts the load and renewable energy fluctuations after introducing disturbances, while Figure 18 shows the output curves of each microsource under these conditions. From the figures, it can be observed that at 5 AM, when the load suddenly increases, distributed generation (DG) increases its output accordingly. At 11 AM, when the load sharply decreases, DG and microturbines (MT) decrease their output, reaching their minimum power output. At 7 AM and 12 PM, when wind turbines (WT) and photovoltaics (PV) generate more power than predicted, DG reduces output to minimize wind curtailment, and batteries charge to minimize solar curtailment, reducing losses. Figures 18 and 19 demonstrate that even in such scenarios, HBOA can find a scheduling solution with significantly lower costs compared to other algorithms.

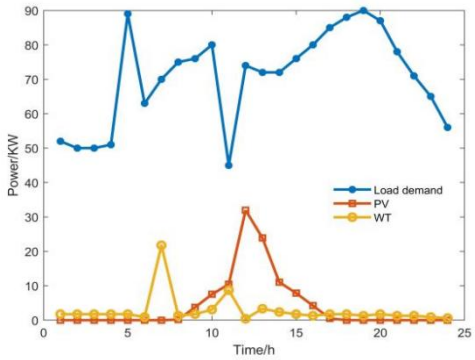

Figure 17. Load and renewable energy fluctuations.

Figure 20 shows the dispatch results of the heterogeneous energy storage strategy in islanded mode for a small-scale commercial microgrid. In the figure, EDLC represents supercapacitors, BS represents batteries and LI represents lithium-ion batteries. It can be observed that at 7 AM, 9 AM and 3 PM, EDLC

rapidly releases a large amount of electrical energy to meet short-term high power demands. Supercapacitors have a fast charge and discharge rate but relatively low energy density, limiting their ability to provide energy for extended periods. On the other hand, both BS and LI can continuously release energy from 3 PM to 10 PM, providing essential power support. However, BS requires a longer charging time compared to LI and is generally used as a backup power source.

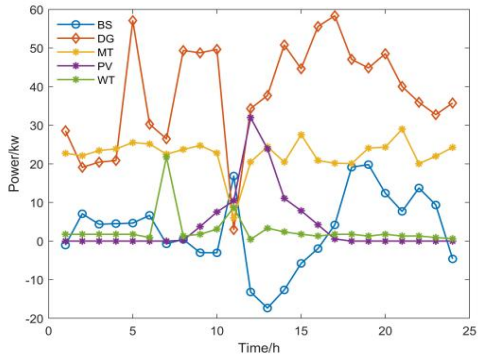

Figure 18. The scheduling results after applying disturbances.

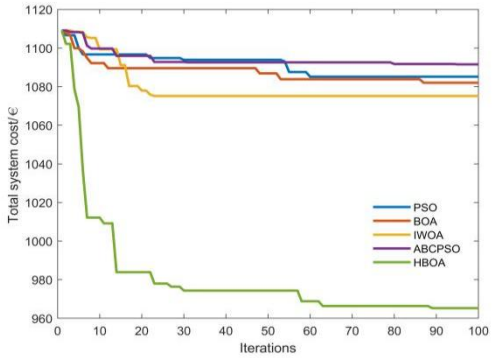

Figure 19. Iteration curve under fluctuating conditions of load and renewable energy sources.

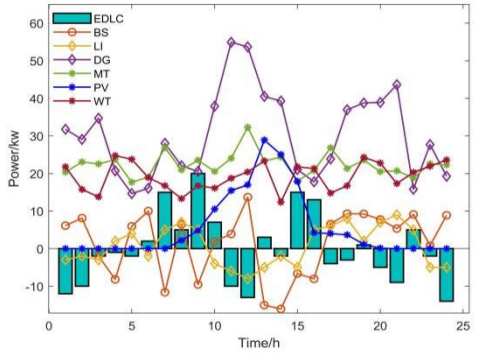

Figure 20. The scheduling results after applying disturbances.

Table 11. Algorithmic results for islanded operation of commercial microgrid with heterogeneous energy storage devices.

Algorithm	Metric	PSO	BOA	IWOA	ABCPSO	**HBOA**
	Best	1488.6545	1492.2847	1432.5279	1494.214	1363.9708
Total system	Worst	1494.2664	1500.9152	1478.8425	1504.7675	1365.0266
cost/€	Mean	1491.3607	1496.9339	1460.8078	1498.464	1364.5545
	Std	2.8113	4.3539	24.7989	5.5684	0.53666

By adjusting the usage strategy under different circumstances, cost savings can be better achieved. Table 11 compares the results of five algorithms for the islanded operation of small-scale commercial microgrid with heterogeneous energy storage devices, and this is contrasted with Table 8. It can be observed that when employing the heterogeneous energy storage strategy, the average system total cost reduced by approximately 1% across all algorithms. Of the five algorithms, HBOA (utilizing the heterogeneous energy storage strategy) achieved the lowest system total cost, and in terms of standard deviation (Std), HBOA exhibited considerable stability, indicating good consistency in its scheduling results under the heterogeneous energy storage strategy.

6. Conclusions

In addressing the optimal economic operation issue in microgrids and the shortcomings of the Butterfly Optimization Algorithm in optimization performance, we proposed a hybrid Butterfly Algorithm. The algorithm utilizes adaptive switch thresholds to balance global exploration and local exploitation capabilities, introduces a diversity learning mechanism to enhance information exchange among populations for improved precision, and presents an elite-directed guiding strategy to accelerate the algorithm's convergence speed. The superiority of the algorithm is validated through numerical simulations on 10 different standard test functions. Additionally, the algorithm's robustness in practical microgrid operations is tested through simulations involving load and renewable energy fluctuations. The study establishes a microgrid model with the objective of minimizing the total system cost and conducts simulations for both islanded and grid-connected operation modes. Comparative analyses with PSO, BOA, IWOA and ABCPSO demonstrate that the Hybrid Butterfly Algorithm (HBOA) achieves a maximum cost reduction of 11.3% in islanded operation and 17.7% in grid-connected operation, ensuring microgrid safety. The algorithm's applicability is further demonstrated through a case study involving a small-scale commercial microgrid, where HBOA yields favorable scheduling results in both operation modes.

Finally, a comparison between the optimal deployment of heterogeneous energy storage and a single storage device in a multi-energy microgrid reveals that the optimal deployment of heterogeneous storage can save operational costs, provide greater system flexibility, and better utilize different energy sources. This approach helps address diverse energy demands and peak-valley variations, enhancing energy utilization efficiency. Moreover, heterogeneous energy storage systems exhibit robustness by adapting energy flow in the face of partial equipment failures or performance degradation, maintaining overall stability in microgrid operations. It should be noted that the advantages of heterogeneous

energy storage may become more apparent in larger-scale, structurally complex microgrids, and further experimental validation of potential benefits will be explored in future work.

Use of AI tools declaration

The authors declare they have not used Artificial Intelligence (AI) tools in the creation of this article.

Conflict of interest

The authors declare there is no conflict of interest.

References

1. R. Chedid, A. Sawwas, D. Fares, Optimal design of a university campus micro-grid operating under unreliable grid considering PV and battery storage, *Energy*, **200** (2020), 117510. https://doi.org/10.1016/j.energy.2020.117510
2. Y. Sun, Y. Meng, L. Ge, Y. Zhang, S. Wang, J. Wang, Application and prospects of artificial intelligence empowering operation optimization in microgrid, *High Voltage Eng.*, **49** (2023), 2239–2252.
3. M. M. Kamal, I. Ashraf, E. Fernandez, Optimal sizing of standalone rural microgrid for sustainable electrification with renewable energy resources, *Sustainable Cities Soc.*, **88** (2023), 104298. https://doi.org/10.1016/j.scs.2022.104298
4. E. Chen, X. Wang, M. Jia, C. Sun, Emergency energy management strategy for cloud energy storage users during planned power outages, *Electr. Power Constr.*, **43** (2022), 72–78.
5. H. Wang, X. Wu, K. Sun, Y. He, Research on the optimal economic power dis-patching of a multi-microgrid cooperative operation, *Energies*, **15** (2022), 8194. https://doi.org/10.3390/en15218194
6. M. N. Hjelmeland, J. Zou, A. Helseth, S. Ahmed, Nonconvex medium-term hydropower scheduling by stochastic dual dynamic integer programming, *IEEE Trans. Sustainable Energy*, **10** (2018), 481–490. https://doi.org/10.1109/TSTE.2018.2805164
7. W. Wei, D. Wu, Z. Wang, S. Mei, J. P. S. Catalão, Impact of energy storage on economic dispatch of distribution systems: A multi-parametric linear programming approach and its implications, *IEEE Open Access J. Power Energy*, **7** (2020), 243–253. https://doi.org/10.1109/OAJPE.2020.3006828
8. G. Cardoso, M. Stadler, A. Siddiqui, C. Marnay, N. DeForest, A. Barbosa-Póvoa, et al., Microgrid reliability modeling and battery scheduling using stochastic linear programming, *Electr. Power Syst. Res.*, **10** (2013), 61–69. https://doi.org/10.1016/j.epsr.2013.05.005
9. M. Hong, X. Yu, N. Yu, K. A. Loparo, An energy scheduling algorithm supporting power quality management in commercial building microgrids, *IEEE Trans. Smart Grid*, **7** (2016), 1044–1056. https://doi.org/10.1109/TSG.2014.2379582
10. M. A. Hossain, H. R. Pota, S. Squartini, A. F. Abdou, Modified PSO algorithm for real-time energy management in grid-connected microgrids, *Renewable Energy*, **136** (2019), 746–757. https://doi.org/10.1016/j.renene.2019.01.005

11. S. Leonori, M. Paschero, F. M. Frattale Mascioli, A. Rizzi, Optimization strategies for Microgrid energy management systems by Genetic Algorithms, *Appl. Soft Comput.*, **86** (2020), 105903. https://doi.org/10.1016/j.asoc.2019.105903
12. R. Torkan, A. Ilinca, M. Ghorbanzadeh, A genetic algorithm optimization approach for smart energy management of microgrids, *Renewable Energy*, **197** (2022), 852–863. https://doi.org/10.1016/j.renene.2022.07.055
13. M. H. Saeed, F. Wang, S. Salem, Y. A. Khan, B. A. Kalwar, A. Fars, Two-stage intelligent planning with improved artificial bee colony algorithm for a microgrid by considering the uncertainty of renewable sources, *Energy Rep.*, **7** (2021), 8912–8928. https://doi.org/10.1016/j.egyr.2021.10.123
14. Q. N. U. Islam, A. Ahmed, S. M. Abdullah, Optimized controller design for islanded microgrid using non-dominated sorting whale optimization algorithm (NSWOA), *Ain Shams Eng. J.*, **12** (2021), 3677–3689. https://doi.org/10.1016/j.asej.2021.01.035
15. A. Almadhor, H. T. Rauf, M. A. Khan, S. Kadry, Y. Nam, A hybrid algorithm (BAPSO) for capacity configuration optimization in a distributed solar PV based microgrid, *Energy Rep.*, **7** (2021),7906–7912. https://doi.org/10.1016/j.egyr.2021.01.034
16. Y. Li, K. Li, Z. Yang, Y. Yu, R. Xu, M. Yang, Stochastic optimal scheduling of demand response-enabled microgrids with renewable generations: An analytical-heuristic approach, *J. Cleaner Prod.*, **330** (2022), 129840. https://doi.org/10.1016/j.jclepro.2021.129840
17. W. Chen, Z. Shao, K. Wakil, N. Aljojo, S. Samad, A. Rezvani, An efficient day-ahead cost-based generation scheduling of a multi-supply microgrid using a modified krill herd algorithm, *J. Cleaner Prod.*, **272** (2020), 122364. https://doi.org/10.1016/j.jclepro.2020.122364
18. Y. Liu, S. Yang, D. Li, S. Zhang, Improved whale optimization algorithm for solving microgrid operations planning problems, *Symmetry*, **15** (2023), 36. https://doi.org/10.3390/sym15010036
19. S. Arora, S. Singh, Butterfly optimization algorithm: A novel approach for global optimization, *Soft Comput.*, **23** (2019), 715–734. https://doi.org/10.1007/s00500-018-3102-4
20. W. Long, T. Wu, M. Xu, M. Tang, S. Cai, Parameters identification of photovoltaic models by using an enhanced adaptive butterfly optimization algorithm, *Energy*, **229** (2021), 120750. https://doi.org/10.1016/j.energy.2021.120750
21. Z. Sadeghian, E. Akbari, H. Nematzadeh, A hybrid feature selection method based on information theory and binary butterfly optimization algorithm, *Eng. Appl. Artif. Intell.*, **97** (2021), 104079. https://doi.org/10.1016/j.engappai.2020.104079
22. A. Lberni, M. A. Marktani, A. Ahaitouf, A. Ahaitouf, Efficient butterfly inspired optimization algorithm for analog circuits design, *Microelectron. J.*, **113** (2021), 105078. https://doi.org/10.1016/j.mejo.2021.105078
23. W. Long, J. Jiao, X. Liang, T. Wu, M. Xu, S. Cai, Pinhole-imaging-based learning butterfly optimization algorithm for global optimization and feature selection, *Appl. Soft Comput.*, **103** (2021), 107146. https://doi.org/10.1016/j.asoc.2021.107146
24. W. Long, M. Xu, J. Jiao, T. Wu, M. Tang, S. Cai, A velocity-based butterfly optimization algorithm for high-dimensional optimization and feature selection, *Expert Syst. Appl.*, **201** (2022), 117217. https://doi.org/10.1016/j.eswa.2022.117217
25. X. Ma, Y. Mu, Y. Zhang, C. Zang, S. Li, X. Jiang, et al., Multi-objective microgrid optimal dispatching based on improved bird swarm algorithm, *Global Energy Interconnect.*, **5** (2022), 154–167. https://doi.org/10.1016/j.gloei.2022.04.013

26. C. Leng, H. Yang, Y. Song, Z. Yu, C. Shen, Expected value model of microgrid economic dispatching considering wind power uncertainty, *Energy Rep.*, **9** (2023), 291–298. https://doi.org/10.1016/j.egyr.2023.05.092
27. H. Zhang, G. Li, S. Wang, Optimization dispatching of isolated island microgrid based on improved particle swarm optimization algorithm, *Energy Rep.*, **8** (2022), 420–428. https://doi.org/10.1016/j.egyr.2022.10.199
28. N. B. Roy, D. Das, Probabilistic optimal power allocation of dispatchable DGs and energy storage units in a reconfigurable grid-connected CCHP microgrid considering demand response, *J. Energy Storage*, **72** (2023), 108207. https://doi.org/10.1016/j.est.2023.108207
29. J. M. Raya-Armenta, N. Bazmohammadi, J. G. Avina-Cervantes, D. Sáez, J. C. Vasquez, J. M. Guerrero, Energy management system optimization in islanded microgrids: An overview and future trends, *Renewable Sustainable Energy Rev.*, **149** (2021), 111327. https://doi.org/10.1016/j.rser.2021.111327
30. S. Hoseinzadeh, D. A. Garcia, L. Huang, Grid-connected renewable energy systems flexibility in Norway islands' Decarbonization, *Renewable Sustainable Energy Rev.*, **185** (2023), 113658. https://doi.org/10.1016/j.rser.2023.113658
31. Y. Li, Z. Zhan, S. Lin, J. Zhang, X. Luo, Competitive and cooperative particle swarm optimization with information sharing mechanism for global optimization problems, *Inf. Sci.*, **293** (2015), 370–382. https://doi.org/10.1016/j.ins.2014.09.030
32. M. K. Naik, R. Panda, A. Wunnava, B. Jena, A. Abraham, A leader Harris hawks optimization for 2-D Masi entropy-based multilevel image thresholding, *Multimedia Tools Appl.*, **80** (2021), 35543–35583. https://doi.org/10.1007/s11042-020-10467-7
33. C. Qu, X. Peng, Memory-encapsulated group algorithm for information sharing, *Pattern Recogni. Artif. Intell.*, **34** (2021), 605–618.
34. Y. Bai, Z. Peng, Tunicate swarm algorithm based on adaptive inertial weight, *Control Decis.*, **37** (2022), 237–246.
35. M. Zhang, D. Long, T. Qin, J. Yang, A chaotic hybrid butterfly optimization algorithm with particle swarm optimization for high-dimensional optimization problems, *Symmetry*, **12** (2020), 1800. https://doi.org/10.3390/sym12111800
36. A. Rezvani, M. Gandomkar, M. Izadbakhsh, A. Ahmadi, Environmental/economic scheduling of a micro-grid with renewable energy resources, *J. Cleaner Prod.*, **87** (2015), 216–226. https://doi.org/10.1016/j.jclepro.2014.09.088
37. G. R. Aghajani, H. A. Shayanfar, H. Shayeghi, Demand side management in a smart micro-grid in the presence of renewable generation and demand response, *Energy*, **126** (2017), 622–637. https://doi.org/10.1016/j.energy.2017.03.051
38. S. Singh, P. Chauhan, N. Singh, Capacity optimization of grid connected solar/fuel cell energy system using hybrid ABC-PSO algorithm, *Int. J. Hydrogen Energy*, **45** (2020), 10070–10088. https://doi.org/10.1016/j.ijhydene.2020.02.018